*IOSR Journal of Mechanical and Civil Engineering (IOSR-JMCE)*
*e-ISSN: 2278-1684, p-ISSN: 2320-334X, Volume 23, Issue 4 Ser. II (Jul. – Aug. 2026), PP 42-48*
*www.iosrjournals.org*

# Dynamic Modeling of Soil Mechanical Behavior: A Numerical Study of Stiffness and Damping Effects

M.I. Ruiz-Sobrevilla[1], J.G. González-Hernández[2,3], C.A. Moreno-Mendoza[2]
J.C. Martínez-Gámez[3], J. Rossette-García[4], V. Jiménez-Zárate[5]
[1]*TecNM Campus Instituto Tecnológico de Cerro Azul, México*
[2] *TecNM Campus Instituto Tecnológico de Ciudad Madero, México*
[3]*Universidad Tecnológica de Altamira, México*
[4]*Universidad Autónoma de Tamaulipas, México*
[5] *TecNM Campus Instituto Tecnológico de Estudios Superiores de Pánuco, México*

***Abstract :***
*The dynamic behavior of soils is relevant to geotechnical, structural, seismic, transportation, and machine-foundation engineering. Although continuum and finite-element formulations provide detailed descriptions of soil behavior, reduced-order models remain valuable for preliminary analysis, parameter identification, control-oriented studies, and real-time simulation. This paper proposes a vertical soil-foundation representation based on an equivalent second-order mass-spring-damper system. The elements considered are the equivalent participating mass, the equivalent damping coefficient the equivalent soil stiffness, and the external force. Three representative conditions (soft, medium, and stiff soil) are numerically evaluated using an equivalent mass of 1000 kg and a 10 kN step load. Stiffness values of $5x10^5$, $2x10^6$, and $8x10^6$ N/m, and damping ratios of 0.20, 0.15, and 0.10 m are considered. The corresponding natural frequencies are 3.56, 7.12, and 14.24 Hz, and the steady-state displacements are 20, 5, and 1.25 mm, respectively. The model provides a transparent framework for studying stiffness and damping effects and is directly implementable in MATLAB/Simulink. It is intended as an equivalent reduced-order model and not as a replacement for nonlinear continuum soil mechanics.*

***Keywords:*** *soil dynamics; second-order dynamic modelling; soil stiffness, damping ratio; soil structure interaction; system identification.*

---

Date of Submission: 09-08-2026 Date of Acceptance: 21-08-2026

---

## I. INTRODUCTION

Dynamic soil response is central to designing structures subjected to earthquakes, machinery, traffic, offshore actions, and other transient loads. Soil-structure interaction (SSI) can modify natural frequencies, damping, displacement demand, and foundation motion; therefore, idealizing a perfectly fixed base can be inadequate when soil flexibility is significant [1] – [4]. Recent full-scale testing also demonstrates that foundation impedance can be experimentally identified from ambient, free, and forced-vibration measurements [5].

A convenient engineering approximation represents the soil-foundation subsystem with lumped stiffness and damping elements. This approach is particularly attractive for system identification, sensitivity analysis, or integration with control and simulation environments. However, experimental research shows that soil stiffness and damping are not universal constants; they depend on strain amplitude, stress state, density, loading frequency, soil composition, and loading history [6] – [12]. Consequently, the parameters of a linear model should be interpreted as equivalent values over a specified operating range.

The objective of this work is to formulate and numerically evaluate a second-order representation of vertical soil-foundation behavior. Three illustrative soil conditions are compared under identical mass and loading. The model is expressed as a differential equation, transfer function, and state-space system, enabling direct implementation in MATLAB/Simulink and providing a baseline for future experimental identification.

## II. THEORETICAL BACKGROUND

The dynamic characterization of soil commonly involves shear modulus and damping ratio. Laboratory resonant-column and cyclic tests show modulus degradation and increasing energy dissipation as strain grows, while confining pressure, density, cementation, reinforcement, and saturation can also affect the response [6] – [13]. Recent measurements on Mexican clays likewise demonstrate the importance of strain-dependent shear modulus and damping for site-response assessment [14], [15].

For a restricted operating range, the vertical soil-foundation response may be represented by an equivalent single-degree-of-freedom system, as shown in Eq. (1):

$$m\ddot{x}(t) + b\dot{x}(t) + kx(t) = f(t) \qquad (1)$$

Where $m, b, k$ $and$ $f$ denote mass, damping, stiffness and force matrices. For nonlinear soil response, stiffness and damping are functions of strain and may also depend on state variables such as effective stress, density, saturation, and loading history. The undamped natural frequency, frequency in hertz, damping ratio, and damped natural frequency are expressed in Eqs. (2) – (5), respectively:

$$\omega_n = \sqrt{\frac{k}{m}} \qquad (2)$$

$$f_n = \frac{\omega_n}{2\pi} \qquad (3)$$

$$\xi = \frac{b}{2\sqrt{km}} \qquad (4)$$

$$\omega_d = \omega_n\sqrt{1-\xi^2} \qquad (5)$$

With zero initial conditions, the transfer function between applied force and displacement is indicated in Eq. (6):

$$G(s) = \frac{X(s)}{F(s)} = \frac{1}{ms^2 + bs + k} \qquad (6)$$

Defining $x_1 = x$ and $x_2 = \dot{x}$, the state-equations became (Eqs. (7)-(8)):

$$\dot{x_1} = x_2 \qquad (7)$$

$$\dot{x_2} = \frac{1}{m}F - \frac{k}{m}x_1 - \frac{b}{m}x_2 \qquad (8)$$

The real soil-foundation impedance can be frequency dependent, with stiffness and damping contributions varying with frequency and foundation configuration [5], [16] – [18]. Thus, the constant-k, constant-b formulation adopted here is a reduced-order approximation suitable for initial modeling and identification.

## III. DEVELOPMENT

A common equivalent participating mass m = 1000 kg and a vertical step force F(t) = 10,000 N were selected. Three soil conditions were defined to isolate the effect of equivalent stiffness and damping. The selected parameters are illustrative and do not represent a particular field site.

*Table 1. Parameters of the three equivalent soil models*

| Soil condition | $k\left(\frac{N}{m}\right)$ | $\xi$ | $b\left(\frac{Ns}{m}\right)$ | $f_n\ (Hz)$ |
|---|---|---|---|---|
| Soft | $5 \times 10^5$ | 0.20 | 8,944.27 | 3.56 |
| Medium | $2 \times 10^6$ | 0.15 | 13,416.41 | 7.12 |
| Stiff | $8 \times 10^6$ | 0.10 | 17,888.54 | 14.24 |

The resulting equations for soft, medium and stiff soil are Eqs. (9)-(11) respectively:

$$1{,}000\ddot{x} + 8{,}944.27\dot{x} + 500{,}000x = f(t) \qquad (9)$$

$$1{,}000\ddot{x} + 13{,}416.41\dot{x} + 2{,}00{,}000x = f(t) \qquad (10)$$

$$1{,}000\ddot{x} + 17{,}888.54\dot{x} + 8{,}000{,}000x = f(t) \qquad (11)$$

The normalized transfer functions are indicated in Eqs. (12) – (14) respectively:

$$G_s(s) = \frac{0.001}{s^2 + 8.9443s + 500} \quad (12)$$

$$G_m(s) = \frac{0.001}{s^2 + 13.4164s + 2000} \quad (13)$$

$$G_r(s) = \frac{0.001}{s^2 + 17.8885s + 8000} \quad (14)$$

Isolating the highest order derivative in Eqs. (11) – (13), Eqs. (15) – (17) are obtained. These equations were implemented in MATLAB/Simulink as shown in Fig. 1. The Function Blocks contain the correspondent Eqs. (14) – (16). The output is the 2nd order derivative (acceleration), then, two integrators in series connection are used to obtain the velocity $\dot{x}(t)$ and the position $x(t)$.

$$\ddot{x} = 0.001f(t) - 8.9443\dot{x} - 500x \quad (15)$$
$$\ddot{x} = 0.001f(t) - 13.4164\dot{x} - 2000x \quad (16)$$
$$\ddot{x} = 0.001f(t) - 17.8885\dot{x} - 8000x \quad (17)$$

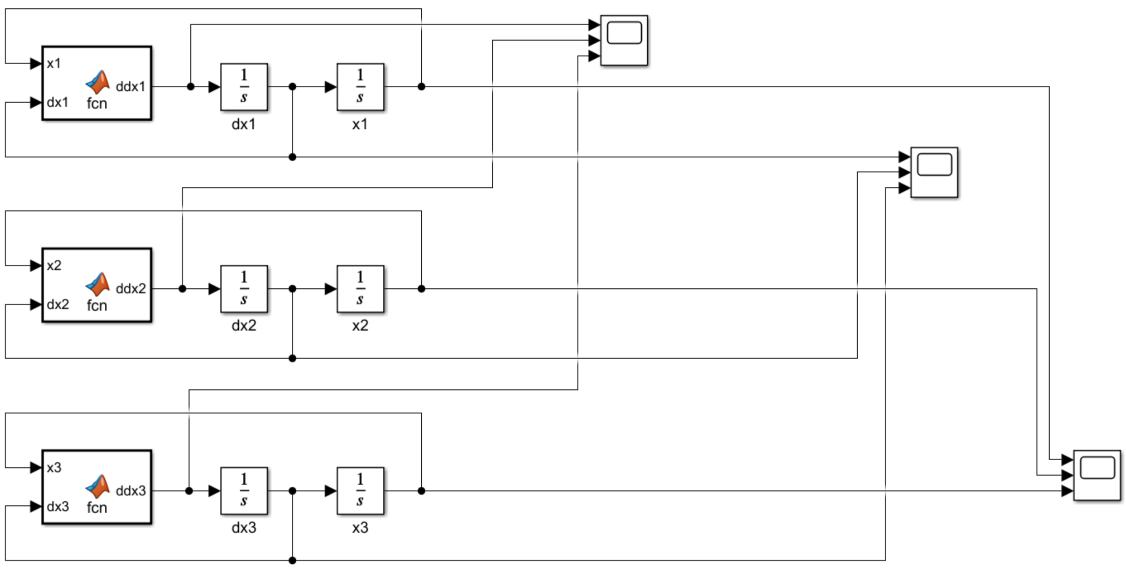


*Figure 1. Block diagram implemented in Simulink for solving the three 2nd order differential equations*

Of course, the general solution can also be obtained by solving Ec. (1). For initial conditions $x(0) = \dot{x}(0) = 0$, and considering a constant force $f(t) = F_0$, then the follow procedure is followed to obtain Ec. (18):

$$x(t) = \mathcal{L}^{-1}\{F(s)G(s)\} = \mathcal{L}^{-1}\left\{\frac{F_0}{s}\left(\frac{1}{ms^2 + bs + k}\right)\right\} = \frac{F_0}{m}\mathcal{L}^{-1}\left\{\frac{1}{s\left(s^2 + \frac{b}{m}s + \frac{k}{m}\right)}\right\}$$

$$x(t) = \frac{F_0}{m}\mathcal{L}^{-1}\left\{\frac{A}{s} + \frac{Bs + C}{s^2 + \frac{b}{m}s + \frac{k}{m}}\right\} = \frac{F_0}{m}\mathcal{L}^{-1}\left\{\frac{A}{s} + \frac{Bs + C}{s^2 + \frac{b}{m}s + \frac{k}{m} + \left(\frac{b}{2m}\right)^2 - \left(\frac{b}{2m}\right)^2}\right\}$$

$$x(t) = \frac{F_0}{m}\mathcal{L}^{-1}\left\{\frac{A}{s} + \frac{Bs + C}{\left(s + \frac{b}{2m}\right)^2 + \frac{k}{m} - \frac{b^2}{4m^2}}\right\} = \frac{F_0}{m}\mathcal{L}^{-1}\left\{\frac{A}{s} + \frac{B\left(s + \frac{b}{2m} - \frac{b}{2m}\right) + C}{\left(s + \frac{b}{2m}\right)^2 + \frac{4mk - b^2}{4m^2}}\right\}$$

$$x(t) = \frac{F_0}{m}\mathcal{L}^{-1}\left\{\frac{A}{s} + \frac{B(s + \alpha - \alpha) + C}{(s + \alpha)^2 + \omega^2}\right\} = \frac{F_0}{m}\mathcal{L}^{-1}\left\{\frac{A}{s} + \frac{B(s + \alpha)}{(s + \alpha)^2 + \omega^2} + \frac{C - B\alpha}{(s + \alpha)^2 + \omega^2}\right\}$$

$$x(t) = \frac{F_0}{m}\mathcal{L}^{-1}\left\{\frac{A}{s} + \frac{B(s+\alpha)}{(s+\alpha)^2+\omega^2} + \frac{1}{\omega}\frac{(C-B\alpha)\omega}{(s+\alpha)^2+\omega^2}\right\}$$

$$x(t) = \frac{F_0}{m}\left(A + e^{-\alpha t}\left(B\cos(\omega t) + \left(\frac{C-B\alpha}{\omega}\right)\sin(\omega t)\right)\right) \tag{18}$$

Where:

$$\omega = \sqrt{\frac{4mk-b^2}{4m^2}}, \alpha = \frac{b}{2m} \tag{19}$$

For obtaining A, B, and C, the following procedure is followed:

$$\left\{\begin{array}{c} \dfrac{1}{s\left(s^2+\frac{b}{m}s+\frac{k}{m}\right)} = \dfrac{A}{s} + \dfrac{Bs+C}{s^2+\frac{b}{m}s+\frac{k}{m}} \\ 1 = A\left(s^2+\frac{b}{m}s+\frac{k}{m}\right) + (Bs+C)s \\ 1 = As^2 + \frac{b}{m}As + \frac{k}{m}A + Bs^2 + Cs \\ 1 = (A+B)s^2 + \left(\frac{b}{m}A + C\right)s + \frac{k}{m}A \end{array}\right\} \tag{20}$$

Equaling common terms:

$$\left\{\begin{array}{c} s^0: \frac{k}{m}A = 1 \therefore A = \frac{m}{k} \\ s^1: \frac{b}{m}A + C = 0 \therefore C = -\frac{b}{m}A = -\frac{b}{m}\left(\frac{m}{k}\right) = -\frac{b}{k} \\ s^2: A + B = 0 \therefore B = -A = -\frac{m}{k} \end{array}\right\} \tag{21}$$

Finaly, substituting the parameters for each case, the resulting time-domain position equations are:

$$x_1(t) = 0.02 - e^{-4.472t}[0.02\cos(21.91t) + 0.004082\sin(21.91t)] \tag{22}$$
$$x_2(t) = 0.005 - e^{-6.708t}[0.005\cos(44.22t) + 0.0007586\sin(44.22t)] \tag{23}$$
$$x_3(t) = 0.00125 - e^{-8.944t}[0.00125\cos(88.99t) + 0.0001256\sin(88.99t)] \tag{24}$$

## IV. RESULTS

For a step force $F_0$, the steady-state displacement is $x_{ss} = \frac{F_0}{k}$, as it can be derived from Ecs. (18) and (21). Therefore, the soft, medium, and stiff models converge to 20, 5, and 1.25 mm, respectively. Because all damping ratios are below unity, the three systems are underdamped and exhibit decaying oscillations before reaching equilibrium.

*Table 2. Main numerical response characteristics*

| Soil | $x_{ss}$ (mm) | $x_{max}$ (mm) | $f_n$ (Hz) | $t_p$ (s) | $v_{max}$ (m/s) | $a(0^+)$ (m/s²) |
|---|---|---|---|---|---|---|
| Soft | 20.00 | 30.53 | 3.56 | 0.143 | 0.338 | 10 |
| Medium | 5.00 | 8.10 | 7.12 | 0.071 | 0.180 | 10 |
| Stiff | 1.25 | 2.16 | 14.24 | 0.035 | 0.096 | 10 |

Figures 2-4 show the comparison among the three graphics of position, velocity, and acceleration in each scenario.

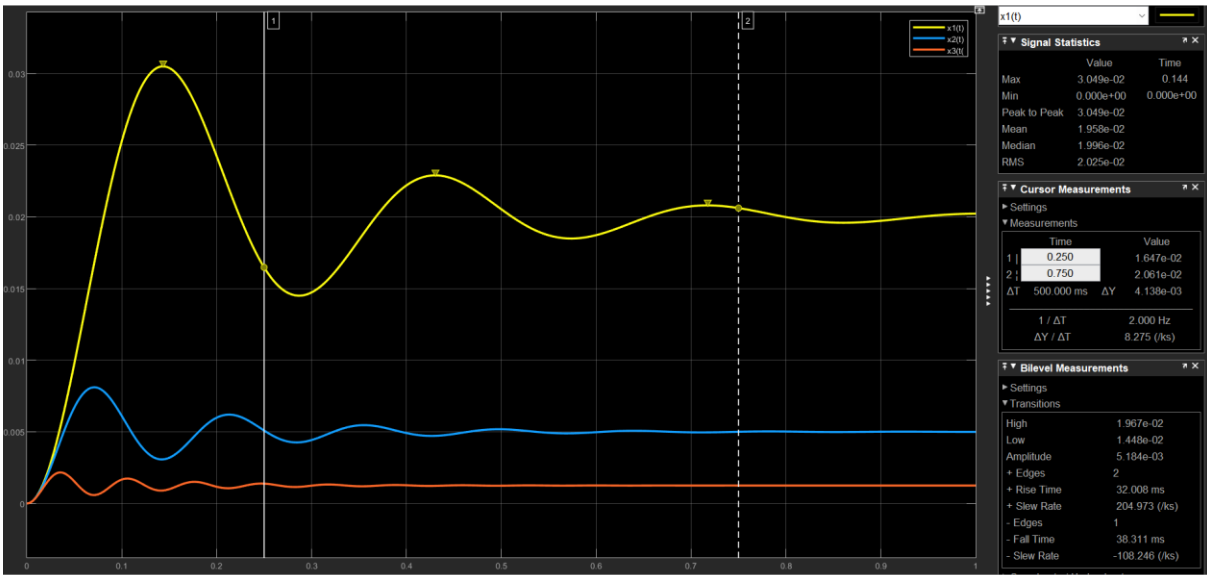


*Figure 2. Position graphics for soft, medium, and stiff soil $x_1(t), x_2(t)$, and $x_3(t)$*

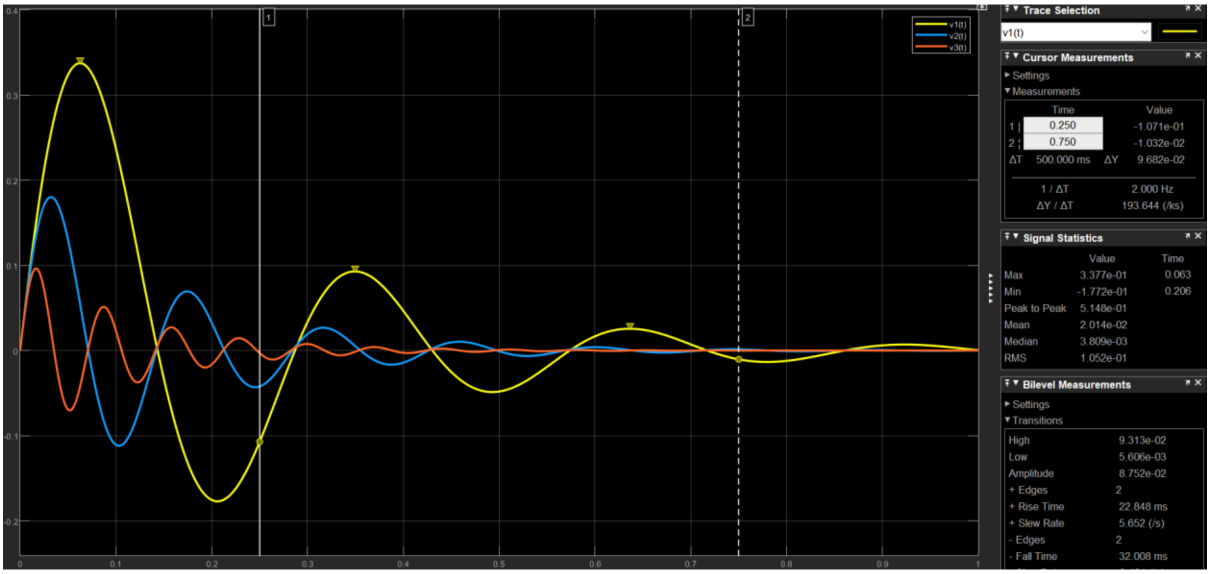


*Figure 3. Velocity graphics for soft, medium, and stiff soil $\dot{x}_1(t), \dot{x}_2(t)$, and $\dot{x}_3(t)$*

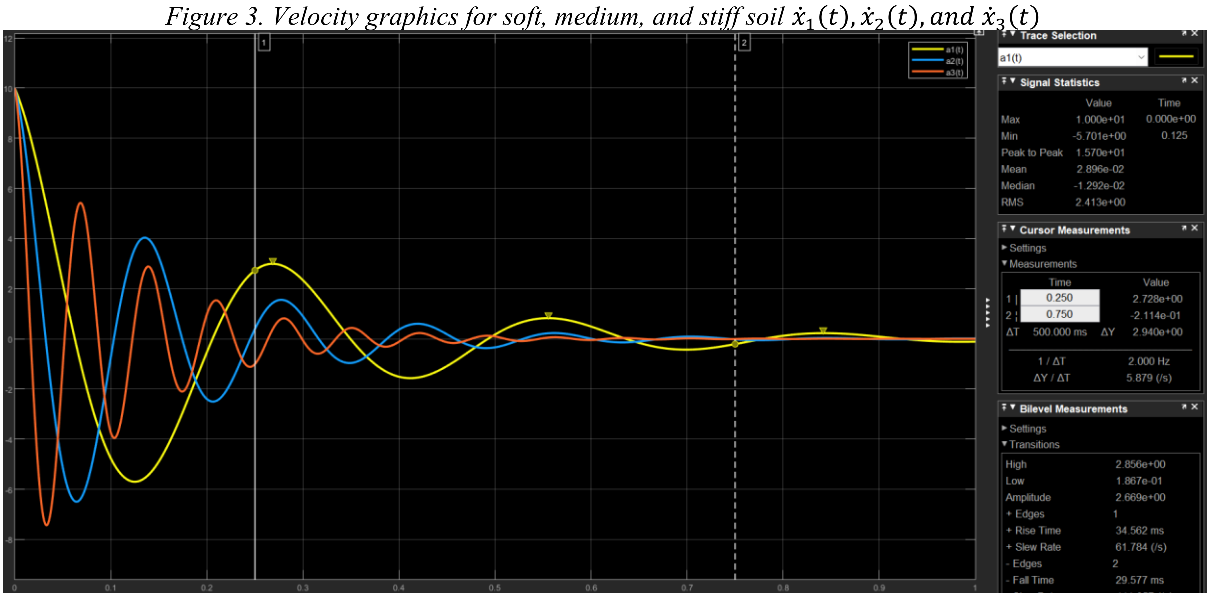


*Figure 4. Acceleration graphics for soft, medium, and stiff soil $\ddot{x}_1(t), \ddot{x}_2(t)$, and $\ddot{x}_3(t)$*

At $t = 0^+$, displacement and velocity are zero. Hence the spring and damping forces initially vanish and all cases satisfy $a(0^+) = \frac{F_0}{m} = 10\ m/s^2$. Their acceleration histories subsequently diverge as stiffness and damping forces develop.

## V. FINDINGS AND COMMENTS

The numerical study highlights four main findings. First, equivalent stiffness strongly controls displacement: the sixteenfold stiffness increase from the soft to stiff case produces a sixteenfold reduction in steady displacement. Second, natural frequency varies with $\sqrt{k}$; consequently, a stiffer soil-foundation representation shifts the dynamic response toward higher frequencies. Third, damping governs the decay of transient oscillations and can be estimated experimentally using resonant-column, free-decay, snap-back, cyclic, or forced-vibration procedures [5] – [9], [16]. Fourth, the model provides a direct connection between geotechnical measurements and system-identification methods.

If an experimental natural frequency is measured and the participating mass is known, an equivalent stiffness can be estimated as $k = m(2\pi f_n)^2$. Once $\xi$ is identified, $b = 2\xi\sqrt{km}$. These relations provide a practical pathway from measured displacement or acceleration records to Simulink parameters.

The principal limitation is linearity. Actual soils exhibit modulus degradation, hysteresis, plasticity, pore-pressure effects, frequency dependence, and permanent deformation. The recent literature confirms that equivalent modulus and damping vary with strain and test conditions [6] – [15]. A logical extension is therefore Eq. (1), or a hysteretic restoring-force model. Frequency-dependent impedance and more elaborate soil-foundation formulations may also be used when the reduced-order assumption becomes insufficient [16] – [20].

## VI. CONCLUSION

An equivalent second-order dynamic model was developed for the vertical response of a soil-foundation system. The formulation is physically interpretable, computationally inexpensive, and directly implementable using differential-equation, transfer-function, or state-space blocks in MATLAB/Simulink.

For the illustrative 1000 kg mass subjected to a 10 kN step force, the soft, medium, and stiff cases produced natural frequencies of 3.56, 7.12, and 14.24 Hz and steady displacements of 20, 5, and 1.25 mm. Increasing stiffness reduces displacement while increasing the characteristic frequency. The damping ratio determines overshoot and the rate of transient decay.

The proposed model should be regarded as a baseline equivalent representation rather than a complete constitutive model of soil. Its principal research value lies in providing a transparent framework for parameter identification and model validation. Future work should experimentally determine $m$, $k$, and $b$; compare the reduced-order model with continuum or finite-element simulations; quantify parameter uncertainty; and introduce nonlinear or frequency-dependent stiffness and damping.

## REFERENCES

[1] B. Bapir, L. Abrahamczyk, T. Wichtmann, and L. F. Prada-Sarmiento, “Soil-structure interaction: A state-of-the-art review of modeling techniques and studies on seismic response of building structures,” Front. Built Environ., vol. 9, Art. no. 1120351, 2023, doi: 10.3389/fbuil.2023.1120351.

[2] F.M. Wani, J. Vemuri, C. Rajaram, and D.V. Babu R, “Effect of soil structure interaction on the dynamic response of reinforced concrete structures,” Natural Hazards Research, vol. 2, no. 4, pp. 304–315, 2022, doi: 10.1016/j.nhres.2022.11.002.

[3] K. Rajkumar, R. Ayothiraman, and V. A. Matsagar, “Effects of soil–structure interaction on dynamic response of framed machine foundation resting on raft and piles,” Pract. Period. Struct. Des. Constr., vol. 26, no. 3, 2021, doi: 10.1061/(ASCE)SC.1943-5576.0000595.

[4] J. I. Boksmati, G. S. Madabhushi, and I. N. Thusyanthan, “Dynamic soil-structure interaction of a shallow founded shear frame and a frame equipped with viscous dampers under seismic loading,” Eng. Struct., vol. 227, Art. no. 111388, 2021, doi: 10.1016/j.engstruct.2020.111388.

[5] C. Amendola, F. de Silva, A. Vratsikidis, D. Pitilakis, A. Anastasiadis, and F. Silvestri, “Foundation impedance functions from full-scale soil-structure interaction tests,” Soil Dyn. Earthq. Eng., vol. 141, Art. no. 106523, 2021, doi: 10.1016/j.soildyn.2020.106523.

[6] F. Qiao, J. Bo, W. Qi, L. Wang, C. Chang, Z. Zhang, and J. Wang, “Study on the dynamic characteristics of soft soil,” RSC Adv., vol. 10, pp. 4630–4639, 2020, doi: 10.1039/C9RA05700E.

[7] O. Doygun and H. G. Brandes, “High strain damping for sands from load-controlled cyclic tests: Correlation between stored strain energy and pore water pressure,” Soil Dyn. Earthq. Eng., vol. 134, Art. no. 106134, 2020, doi: 10.1016/j.soildyn.2020.106134.

[8] K. Mog and P. Anbazhagan, “Evaluation of the damping ratio of soils in a resonant column using different methods,” Soils Found., vol. 62, no. 1, Art. no. 101091, 2022, doi: 10.1016/j.sandf.2021.101091.

[9] H. Gao et al., “Dynamic shear modulus and damping of cemented and uncemented lightweight expanded clay aggregate (LECA) at low strains,” Soil Dyn. Earthq. Eng., vol. 142, Art. no. 106555, 2021, doi: 10.1016/j.soildyn.2020.106555.

[10] A. Baghbani, T. Choudhury, P. Samui, and S. Costa, "Prediction of secant shear modulus and damping ratio for an extremely dilative silica sand based on machine learning techniques," Soil Dyn. Earthq. Eng., vol. 165, Art. no. 107708, 2023, doi: 10.1016/j.soildyn.2022.107708.

[11] S. Rohilla, and R. Sebastian, "Resonant column and cyclic torsional shear tests on Sutlej River sand subjected to the seismicity of Himalayan and Shivalik hill ranges: A case study," Soil Dyn. Earthq. Eng., vol. 166, Art. no. 107766, 2023, doi: 10.1016/j.soildyn.2023.107766.

[12] L. Zhang, J. Shi, Q. Peng, and C. Chen, "Dynamic behavior of Haikou marine clay treated with cement," Constr. Build. Mater., vol. 405, Art. no. 133320, 2023, doi: 10.1016/j.conbuildmat.2023.133320.

[13] A. Shafiee et al., "Modulus reduction and damping characteristics of geotextile-reinforced sands," Soil Dyn. Earthq. Eng., vol. 181, Art. no. 108641, 2024, doi: 10.1016/j.soildyn.2024.108641.

[14] V. M. Taboada-Urtuzuástegui et al., "Dynamic properties of clay for earthquake response analysis in the Bay of Campeche," Ing. Sísmica, no. 109, pp. 47–68, 2022, doi: 10.18867/RIS.109.596.

[15] A. Fernández-Lavín, E. Ovando-Shelley, and C. Chamorro-Zurita,"Damping ratio on lacustrine soils using the wavelet transform" Soil Dyn. Earthq. Eng., vol. 180, Art. no. 108583, 2024, doi: 10.1016/j.soildyn.2024.108583.

[16] F. de Silva, C. Amendola, D. Pitilakis, and F. Silvestri, "A comparative study on the interpretation procedure of field tests for measuring the dynamic impedance of a surface footing," J. Earthq. Eng., vol. 27, no. 11, pp. 2970–2993, 2023, doi: 10.1080/13632469.2022.2121334.

[17] F. De-Silva, C. Amendola, D. Pitilakis, and F. Silvestri, "Prediction of foundation stiffness and damping ratio under horizontal translation and rocking motion," Soil Dyn. Earthq. Eng., vol. 166, Art. no. 107735, 2023, doi: 10.1016/j.soildyn.2022.107735.

[18] H. D. B. Aji et al., "Dynamic impedance and compliance surfaces of twin adjacent surface foundations under synchronous and asynchronous loads," Soil Dyn. Earthq. Eng., vol. 182, Art. no. 108740, 2024, doi: 10.1016/j.soildyn.2024.108740.

[19] G. Tekin and S. Gencer, "The dynamic soil–foundation–structure interaction problem in the time domain using a discrete element model," Appl. Sci., vol. 14, no. 23, Art. no. 10994, 2024, doi: 10.3390/app142310994.

[20] L. Auersch, "Soil–structure interaction and damping by the soil—Effects of foundation groups, foundation flexibility, soil stiffness and layers," Vibration, vol. 8, no. 1, Art. no. 5, 2025, doi: 10.3390/vibration8010005.